Fate of [^{14}C]Emamectin Benzoate in Head Lettuce

Louis S. Crouch* and William F. Feely

Department of Drug Metabolism II, Merck Research Laboratories, P.O. Box 450, Hillsborough Road, Three Bridges, New Jersey 08887

The fate of [^{14}C]emamectin benzoate in head lettuce was investigated. Two treatment groups, at a 1× (0.015 lb of active ingredient/acre) or a 5× rate, received eight weekly applications. Plants were harvested from 2 h to 10 days after the last application. Total carbon-14 residue in foliage declined from ~360 to 80 ppb (1×) or 1600 to 600 ppb (5×). Approximately 75–90% of the total carbon-14 residue was extractable with cold solvents. The parent (3–33% of extractable residue) and eight degradates were tentatively identified by HPLC, but the major portion of the extractable residue was an unidentified polar fraction (28–78% of extractable residue). These polar extractable residues were not conjugates and were of a complex nature. Portions of the unextractable residue (equivalent to 5–10% of total residue each) were extractable with hot dimethyl sulfoxide, incorporated into glucose released by acid hydrolyis, or remained uncharacterized as bound residue.

Keywords: *Emamectin; MK-0244; avermectin; metabolism; lettuce*

INTRODUCTION

Emamectin benzoate is the generic name for the benzoic acid salt of the experimental avermectin insecticide 4″-deoxy-4″-*epi*-(methylamino)avermectin B_1 (MAB1, MK-0244, CAS 137512-74-4), which is a mixture of two active compounds: 4″-deoxy-4″-*epi*-(methylamino)avermectin B_{1a} (MAB1A) and 4″-deoxy-4″-*epi*-(methylamino)avermectin B_{1b} (MAB1B). These compounds, which are homologous semisynthetic macrolides of ~900 molecular weight (Figure 1), are derived from the natural fermentation products avermectins B_{1a} and B_{1b} (from *Streptomyces avermitilis*) by replacement of the 4″-hydroxyl constituent with an epi-*N*-methyl group. The MAB1A homologue constitutes no <90% of the active ingredient, whereas the MAB1B homologue constitutes no >10%. The application rates for the active ingredient (ai) are calculated on the basis of these salts.

Abamectin, a mixture of the natural avermectins B_{1a} and B_{1b}, is currently in worldwide use as a miticide/insecticide on various crops including citrus, cotton, vegetables, fruit, and ornamentals. Emamectin benzoate is an effective larvacide against lepidoptera (Trumble et al., 1987) and is being developed for use on a number of crop types.

The goal of this study was to characterize the terminal residue of emamectin benzoate in mature plants of a typical market variety of head lettuce grown, treated, and harvested under conditions simulating the proposed field use of the compound. Two plots of plants were treated with seven applications of the benzoate salt of [^{14}C]MAB1A and an eighth application with the benzoate salt of [^{3}H/^{14}C]MAB1A, at either 0.015 or 0.075 lb of ai/acre (17 or 85 g/ha).

MATERIALS AND METHODS

Test Compounds. The test compounds used in this study were ^{14}C- and ^{3}H-labeled MAB1A benzoate and were provided by the Labeled Compound Synthesis Group, Department of Drug Metabolism II, Merck Research Laboratories, Rahway, NJ. The [^{14}C]MAB1A was labeled at one of five positions (C3, C7, C11, C13, or C23) per molecule (Figure 1) and was supplied at a specific activity (sp act.) of 29.06 mCi/mmol or 63 980 dpm/μg of MAB1A benzoate. The [^{3}H]MAB1A benzoate (labeled at 5 H, Figure 1) was supplied with a sp act. of 282.2 mCi/mmol or 621 600 dpm/μg. The test compounds were prepared for application by dissolving them in a vehicle (a proprietary agricultural formulation) and diluting with water. For the last application to the 1× and 5× plots, [^{3}H]MAB1A was added to the [^{14}C]MAB1A benzoate to give a sp act. of 46 205 dpm of tritium and 59 232 dpm of carbon-14 per microgram of MAB1A benzoate. The test compound concentration was nominally 60 (1× plot) or 300 (5× plot) ppm after dilution with water for application to the plants. The radiopurity of the [^{3}H]- and [^{14}C]-MAB1A in the application solutions was ~95%.

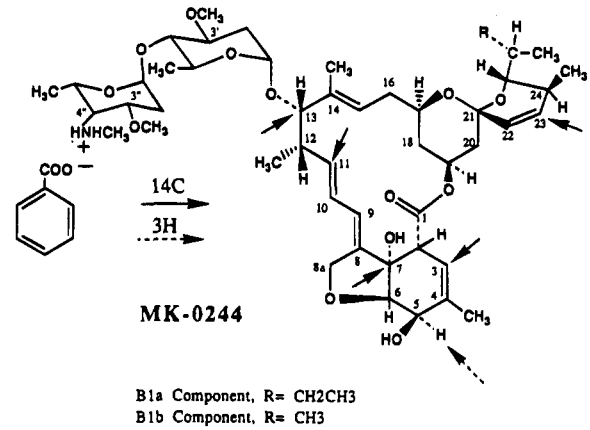

Figure 1. Emamectin benzoate structure. Structure of major (4″-deoxy-4″-*epi*-(methylamino)avermectin B_{1a}, MAB1A) and minor (4″-deoxy-4″-*epi*-(methylamino)avermectin $B1_b$, MAB1B) homologues of emamectin benzoate (MK-0244).

Lettuce Cultivation. The head lettuce was of the Great Lakes variety. The plants were grown in stock tanks (3 ft × 8 ft × 24 in. ~20 sq ft) buried to a depth of ~18 in. and containing sandy loam soil. The two test plots and a control plot were located in an outdoor shelter (ABC Laboratories, Columbia, MO) with four screened sides and covered with a Filon plastic roof. The Filon roof immediately above the three lettuce plots was removed 2 weeks prior to the first harvest date. A removable roof of translucent plastic sheeting was constructed and the plants were directly exposed to full sunlight daily between ~8 a.m. and 4 p.m.; during periods of

* Author to whom correspondence should be addressed (e-mail louis_crouch@merck.com).

0021-8561/95/1443-3075$09.00/0

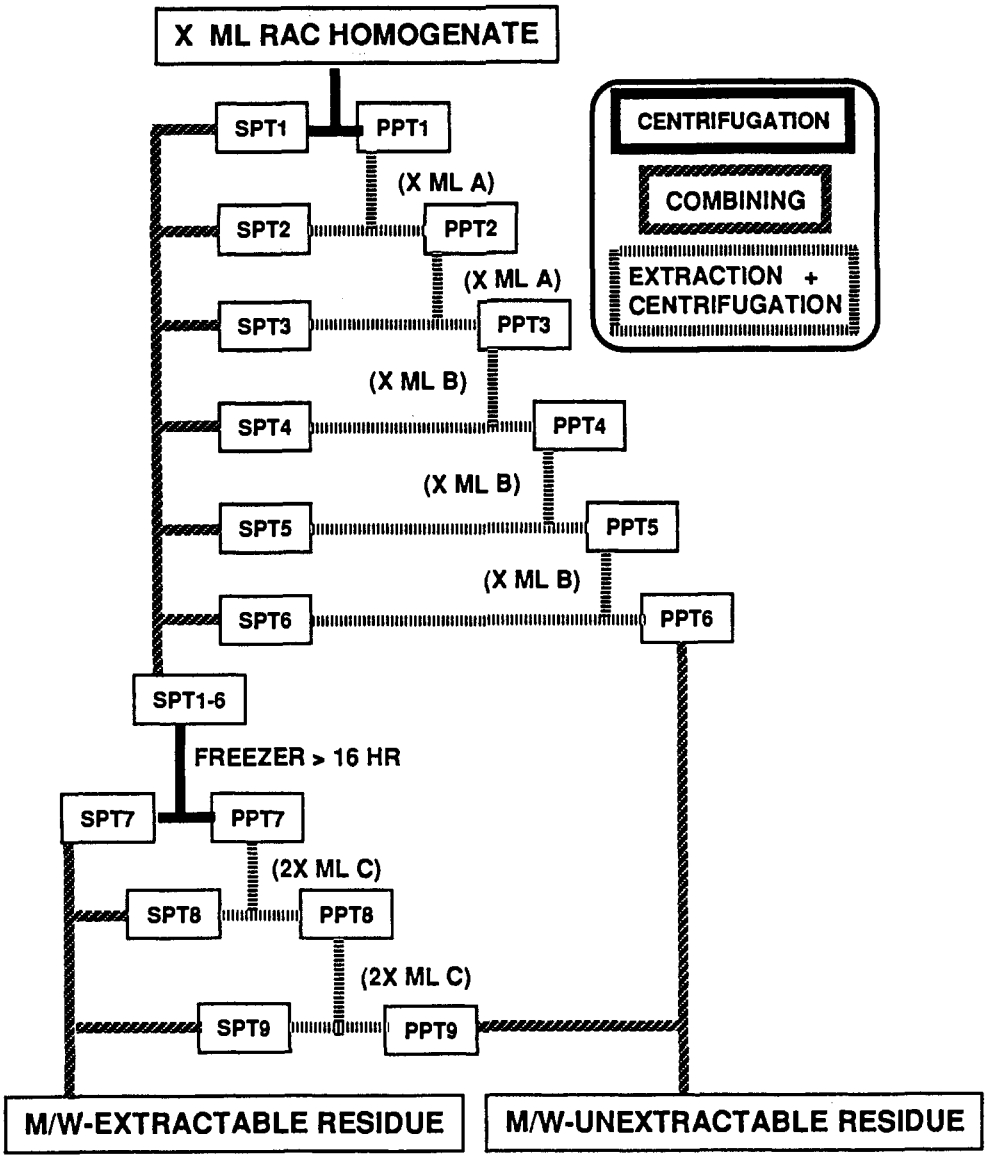

Figure 2. M/W extraction scheme for lettuce RAC. The methanol homogenates of the RAC (x mL = volume of homogenate) were extracted with indicated volumes of **A** (1 mM ammonium acetate in methanol), **B** (5 mM ammonium acetate in 50% methanol), and **C** (methanol). Key: SPT = supernatant; PPT = precipitate.

rainfall and between the hours of ~4 p.m. and 8 a.m. the plants were covered with the plastic sheeting. The period from first application of [^{14}C]MAB1A to the end of harvesting occurred between April 24 and June 22, 1990.

Lettuce Treatment and Harvest. The plants in the 1× and 5× plots were treated once weekly beginning at the two-leaf stage and continuing over 7 weeks to maturity; plants in the control plot were untreated. Applications were made with a CO_2-powered sprayer. Plants were harvested at 2 h and 1, 3, 7, and 10 days following the 8th and final application of radiolabeled MAB1A. Three plants from each plot were selected at random at each preharvest interval (PHI) for a total of 15 plants from each plot. At harvest, the dead leaf and roots were removed from the foliage of each plant. The foliage, or raw agricultural commodity (RAC), was then separated into two fractions: wrapper leaves and head. The four sample types (dead leaf, roots, wrapper leaf, and head) from the control plants at each PHI were composited.

Sample Storage and Processing. The dead leaf and roots were placed in a freezer on the day of harvest and stored frozen until processed. The RAC fractions, consisting of the wrapper leaf and head, were stored in a refrigerator for 1–2 days until processing. The leaves from the heads were detached, and the individual leaves of each RAC fraction from each plant from the 1× and 5× plots were rinsed separately three times with a methanol spray to remove surface residues. A total of ~500 mL was used for the total wrapper or head leaf per plant during each rinse. For the control plants, the wrapper leaves and head leaves were composited prior to rinsing with methanol. The resultant four processed specimens of the RAC from the individual 1× or 5× plants or the composited control plants (rinsed head leaf, rinsed wrapper leaf, wrapper leaf rinse, and head leaf rinse) were stored in a freezer until further processing or analysis.

The rinsed head and wrapper leaf, and dead leaf samples from the 1× and 5× plants were thawed and minced with scissors. Each specimen was then homogenized with ~1–2 mL of methanol per gram of specimen using a Brinkmann Polytron, and the weight of the homogenate was determined. The root specimens were thawed, placed in 50 mL water in a 250 mL bottle, shaken, and drained to remove soil prior to mincing and homogenization as just described for the leaf specimens, except that ~4 mL of methanol to every 1 g of specimen was used. All methanol homogenates were stored in a freezer until analysis or extraction.

Methanol/Water Extraction of the RAC. Aliquots of each of the four fractions of the RAC (wrapper leaf rinse, head leaf rinse, homogenized rinsed wrapper leaf, and homogenized rinsed head leaf) from individual plants that were equal to 2% of each total rinse volume or total homogenate weight were combined to give the equivalent of a methanol homogenate representing 2% of each RAC. These methanol homogenates

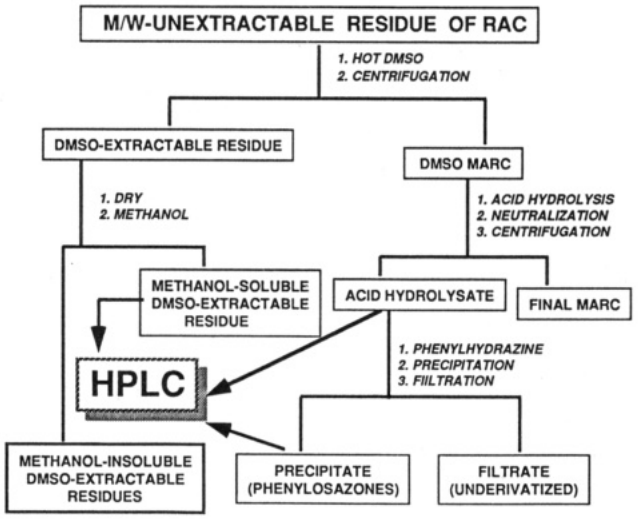

Figure 3. Fractionation of M/W unextractable residue of lettuce RAC. General scheme for fractionation of M/W unextractable residue of lettuce RAC and subsequent characterization of subfractions by derivatization and/or HPLC.

of the RACs from individual 1× or 5× plants were then subjected to a methanol/water (M/W) extraction procedure at room temperature (Figure 2). The extraction resulted in the extractable residues and the M/W marcs (M/W unextractable residue) of the RACs. For some studies, the methanol homogenates resulting from the combination of the four processed fractions of the RAC of each plant as just described were further composited according to rate (1× or 5×) and PHI using all three plants from each PHI.

DMSO Extraction of the RAC M/W Marc. The procedures used for hot dimethyl sulfoxide (DMSO) extraction were similar to those in previous plant studies (Feely and Wislocki, 1991; Haque et al., 1976). The marcs remaining after M/W extraction (Figure 2) of composited 5× plants (3 plants each, 3 and 7 days PHI) and untreated plants (7 days PHI) were dried by first placing them on a warm hot plate for ~6 h followed by drying overnight with a heat lamp. The dried M/W marc was extracted with hot (~70–80 °C) DMSO (~200 mg marc per 100 mL of DMSO) for 22 h. The supernatant was removed after centrifugation. The tubes containing the precipitates were reextracted with ~30 mL of methanol, the extract was centrifuged, and the supernatant was removed and combined with the DMSO extract. The precipitate was reextracted with ~30 mL of DMSO, the extract was centrifuged, and the second DMSO supernatant was combined with the other two extracts to give the DMSO-extractable residue of the M/W marc (Figure 3).

Acid Hydrolysis of the RAC DMSO Marcs. Acid hydrolysis of the DMSO marcs was performed similarly to methods previously described (Feely and Wislocki, 1991; Honeycutt and Adler, 1975). The DMSO marcs from the composited RAC of 5× plants (3 and 7 days PHI) were hydrolyzed by addition of ~1 mL of 70% sulfuric acid per 100 mg of marc. The samples were then chilled overnight in a refrigerator, diluted (10-fold) with water, and refluxed for 4 h the next day. The acid hydrolysis solutions were adjusted to pH ~7 with potassium hydroxide as monitored by an Orion model 420A pH meter and then were centrifuged. The supernatant (acid hydrolysate) was removed, leaving the final marc (Figure 3). The DMSO marc of the RAC from untreated plants was subjected to the same acid hydrolysis procedure after addition of ~4 ng of [^{14}C]glucose (Sigma, sp act. = 4 mCi/mmol or 4.93 × 10^7 dpm/μg) per 20 mg of DMSO marc just prior to the addition of 70% sulfuric acid or just after neutralization.

Derivatization of Glucose in Acid Hydrolysates. The derivatization of glucose in the acid hydrolysates of the DMSO marcs was performed by methods similar to those previously described (Feely and Wislocki, 1991; Honeycutt and Adler, 1975). The neutralized acid hydrolysates of the DMSO marcs from the treated plants and the [^{14}C]glucose-added DMSO marcs from untreated plants (equivalent to ~10 mg of marc) were refluxed with 100 mg of phenylhydrazine and 150 mg of sodium acetate for ~7 h and then placed in a refrigerator overnight. The mixture was then filtered through Whatman No. 54 filter paper to remove the yellow precipitate (osazones). The filtered osazones were rinsed with water and then dissolved in methanol; the yellow precipitate adhering to glass after precipitation was rinsed with water, solubilized with methanol, and combined with the filtered osazones (Figure 3).

Quantitation of Total Radioactivity in Homogenates, Extracts, Acid Hydrolysates, Osazones, and Marcs. The total radioactivity in homogenates of roots, dead leaf, and RAC or RAC fractions (except rinsed head leaf) and in all marcs (M/W, DMSO, and final) was determined by radiocombustion analysis (RCA). All RCA was performed by oxidation in a Packard model B306 or 307 sample oxidizer followed by liquid scintillation counting in a Packard model 460 or 4530 counter with external standardization for quench correction. Packard Permafluor and Monophase S were used as scintillation cocktails for carbon-14 and tritium, respectively. The quench curves were stored by the counters for automatic conversion of cpm data to dpm. The dpm data obtained from RCA were corrected for recovery from the oxidizers by comparison of unoxidized versus oxidized standards.

The total radioactivity in all extracts (M/W, DMSO), the homogenates of head leaf, the acid hydrolysates of the DMSO marc, and the phenylosazones from derivatization of the acid hydrolysates was determined by liquid scintillation counting (LSC) using the same scintillation counters as for the RCA, but with Packard Instagel as the scintillation cocktail. Also, the dual isotope mode programs of the counters were used as all specimens contained ^{14}C- and ^{3}H-residues. It was found that the LSC and RCA assays gave similar results for total radioactivity in RAC homogenates (data not shown).

HPLC Methods for Extractable Residue. The HPLC equipment for all methods consisted of a Hewlett-Packard model 1040A diode array detector, Hewlett-Packard 1040M data station, Spectra-Physics SP8800 solvent delivery system, Rheodyne 7125 injector, and a Pharmacia Frac-100 fraction collector (system 1) or a Hewlett-Packard model 1040A diode array detector, Hewlett-Packard 85B data station, Spectra-Physics SP8700 solvent delivery system, Rheodyne 7125 injector, and a Pharmacia Frac-100 fraction collector (system 2). The eluate UV profile for all methods was monitored at 210 (or 220), 245, and 280 nm and peak spectra were obtained from 200–400 nm by the diode array detectors. The HPLC solvents for all methods were of HPLC grade and water was purified to 18 MΩ resistance with a Waters Milli-Q system. All HPLC methods were performed at room temperature, and fractions of eluate (1 min) were collected in scintillation vials. The eluate fractions or aliquots from the eluate fractions were then mixed with 4–5 mL of Packard Instagel, and the dpm was determined with a dual isotope program on the LSC equipment as just described for quantitation of total radioactivity.

The extractable residue from the RAC of each individual 1× and 5× plant was analyzed by HPLC using a C18 column (C18HPLC) by the C18HPLC Method 1 as follows: An Axxiom (Axxi-Chrom C18, particle size of 5 μm, 4.6 × 250 mm) column, 5 mM ammonium acetate (NH_4Ac; Chemical Dynamics or Sigma) in water (solvent A, not pH-adjusted), and 5 mM NH_4-Ac in methanol (solvent B); flow rate = 1 mL/min; gradient = 85% B from 0 to 35 min, 85 to 100% B from 35 to 50 min, and 100% B from 50 to 60 min). Aliquots of the M/W-extractable residue were chromatographed with the following standards (~1–5 μg each): avermectin B_{1a} monosaccharide (MSB1A), 4″-deoxy-4″-*epi*-(*N*-formyl)avermectin B_{1a} (FAB1A), 4″-deoxy-4″-*epi*-(*N*-formyl-*N*-methyl)avermectin B_{1a} (MFB1A), 14-exomethylene-15-hydroxy-4″-deoxy-4″-*epi*-(methylamino)-avermectin B_{1a} (15OH-MAB1A), 8a-oxo-4″-deoxy-4″-*epi*-(methylamino)avermectin B_{1a} (8AOXO-MAB1A), 8a-hydroxy-4″-deoxy-4″-*epi*-(methylamino)avermectin B_{1a} (8AOH-MAB1A), 4″-deoxy-4″-*epi*-aminoavermectin B_{1a} (AB1A), and 8,9-Z-4″-deoxy-4″-*epi*-(methylamino)avermectin B_{1a} (8,9-Z-MAB1A) (Figure 4).

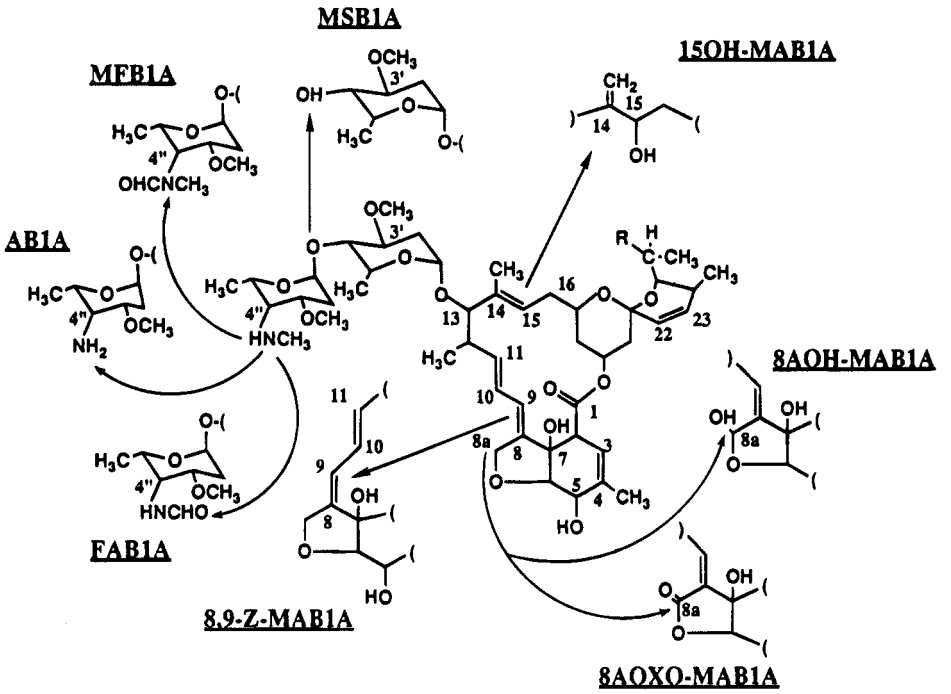

Figure 4. Structures of avermectin standards. Residue components in MAB1A-treated lettuce identified by HPLC cochromatography with standards. MSB1A = avermectin B_{1a} monosaccharide; FAB1A = 4″-deoxy-4″-*epi*-(*N*-formyl)avermectin B_{1a}; MFB1A = 4″-deoxy-4″-*epi*-(*N*-formyl-*N*-methyl)avermectin B_{1a}; 15OH-MAB1A = 14-exomethylene-15-hydroxy-4″-deoxy-4″-*epi*-(methylamino)avermectin B1a; 8AOXO-MAB1A = 8a-oxo-4″-deoxy-4″-*epi*-(methylamino)avermectin B_{1a}; 8AOH-MAB1A = 8a-hydroxy-4″-deoxy-4″-*epi*-(methylamino)avermectin B_{1a}; AB1A = 4″-deoxy-4″-*epi*-aminoavermectin B1a; MAB1A = 4″-deoxy-4″-*epi*-(methylamino)avermectin B_{1a}; 8,9-*Z*-MAB1A = 8,9-*Z*-4″-deoxy-4″-*epi*-(methylamino)avermectin B_{1a}.

Confirmation of the identity of nine components of the extractable residue of the RAC (MAB1A and its primary degradates: MSB1A, FAB1A, MFB1A, 15OH-MAB1A, 8AOXO-MAB1A, 8AOH-MAB1A, AB1A, and 8,9-Z-MAB1A ; see Figure 4) was achieved with the composited RAC from plants treated at the 5× rate, 3 days PHI. The residue was first chromatographed with the standards by C18HPLC Method 1, and the eluate fractions corresponding to the UV peak(s) of the standards were combined and reassayed by either one of two additional HPLC methods. The first method (SIHPLC) used a silica column (Axxiom Axxi-Chrom silica, particle size of 5 μm, 4.6 × 250 mm) with the following conditions: eluents, solvent A = isooctane with 0.4 mM triethylamine (TEA); solvent B = ethanol with 0.4 mM TEA; flow rate = 1 mL/min; gradients for 0−40 min = 10−20% B and for 40−60 min = 20% B. The second method (CATHPLC) used a C8/cation exchange column (Alltech RP-8/cation, particle size 7 μm, 4.6 × 250 mm column) with the following conditions: eluents, solvent A = water with 50 mM NH_4Ac at pH 5.5; solvent B = methanol with 50 mM NH_4Ac; flow rate = 1 mL/min; gradients for 0−30 min = 75% B and for 30−50 min = 75−100% B.

The polar residues were obtained by HPLC of the extractable residue of the RAC from composited 5× plants (3 days PHI) for additional characterization by HPLC and for enzymatic and acid treatment. The polar residues were defined as all radioactivity that eluted prior to the most polar avermectin standard used (MSB1A) when chromatographed on a C18 column eluted with M/W containing NH_4Ac, such as C18HPLC Method 1. The polar residues were obtained by one of two HPLC methods, that is, the C18HPLC Method 1 or by C18HPLC Method 2. The latter uses a semipreparative C18 column (Axxiom Axxi-Chrom C18, particle size of 5 μm, 10 × 250 mm) with the following conditions: solvent A = water with 5 mM NH_4Ac (not pH-adjusted); solvent B = methanol with 5 mM NH_4Ac; flow rate = 3 mL/min; and gradients for 0−35 min = 85−90% B, for 35−40 min = 90−100% B, and for 40−50 min = 100% B.

The polar residues were subjected to additional HPLC methods in an attempt to resolve individual residue components. First, the polar residues were fractionated with a C18 column (Phenomenex ODS-30, 7 μm particle size, 4.6 × 250 mm) by C18HPLC Method 3 with the following conditions: solvent A = water with 5 mM NH_4Ac (not pH-adjusted); solvent B = methanol with 5 mM NH_4Ac; flow rate = 1 mL/min; and gradients for 0−50 min = 10−100%B and for 50−70 min = 100% B. One-minute fractions of eluate were collected and the 60 fractions were pooled into 10 fractions by combining the eluate fractions consecutively, beginning with the first fraction, so that each of the 10 pooled fractions contained ~10% of the total eluted radioactivity. Each of these 10 fractions of polar residues was then assayed by another HPLC method (DIOLHPLC) with a diol column (E. Merck HiBar Lichrosphere; particle size of 5 μm, 4.6 × 250 mm) with the following conditions: eluents, solvent A = hexane:methylene chloride (2:1) containing acetic acid (0.1%) and TEA (0.4 mM), solvent B = methanol containing acetic acid (0.1%) and TEA (0.4 mM); flow rate = 1 mL/min; and gradients for 0−30 min = 0−25% B, for 30−60 min = 25−100% B, and for 60−90 min = 100% B.

Enzymatic Treatment of Polar Residues. Enzymatic treatment of polar residues was performed with α-glucosidase (AGLU; Sigma Type I, sp act. = 10.5 units/mg protein for *p*-nitrophenylglucose), β-glucosidase (BGLU, sp act. = 4.8 units/mg protein for salicin), and β-glucuronidase (BGLC, Sigma Type VIII-A, sp act. = 7600 units/mg protein for phenolphthalein glucuronide).

The reaction conditions for incubation with AGLU were AGLU (1 unit), polar residues (~80 ng MAB1A equivalents) in 1 mL of 0.1 N sodium acetate (NaAc), pH 6.8. The incubation was performed at room temperature for 17 h at which time the reaction was stopped by vortexing with 1 mL of methanol. Under these reaction conditions, 500 μg of *p*-nitrophenyl α-D-glucopyranoside (PNP-GLU, Sigma) was completely hydrolyzed to PNP (data not shown).

The reaction conditions for incubation with BGLU were BGLU (1 unit), polar residues (~80 ng MAB1A equivalents) in 1 mL of 0.1 N NaAc, pH 5.0. The incubation was performed at room temperature for 17 h at which time the reaction was stopped by vortexing with 1 mL of methanol. Under these reaction conditions, 500 μg of salicin (Sigma) was completely hydrolyzed (data not shown).

The reaction conditions for incubation with BGLC were BGLC (10 units), polar residues (~80 ng MAB1A equivalents)

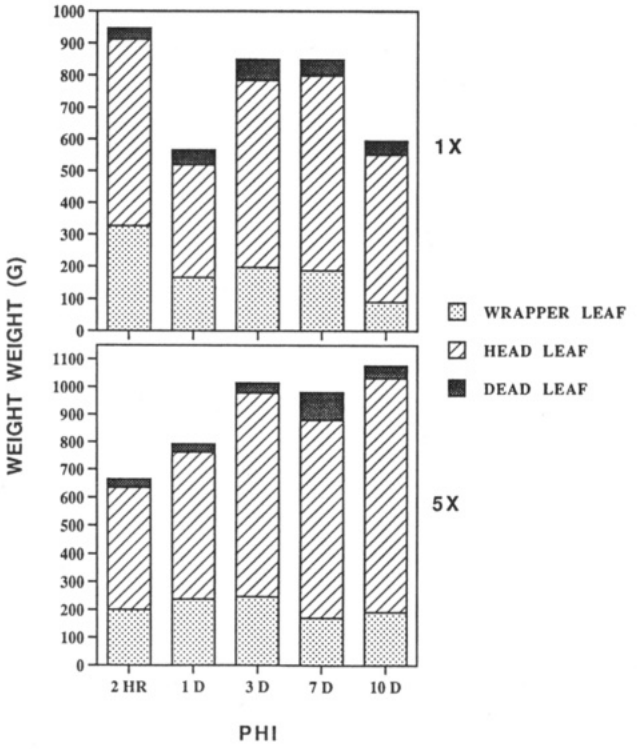

Figure 5. Wet weights of lettuce leaf types at harvest. Values are mean wet weight (g) for three plants per PHI and application rate.

in 1 mL of 0.1 N NaAc, pH 6.8. The incubation was performed at room temperature for 17 h at which time the reaction was stopped by vortexing with 1 mL of methanol. Under these reaction conditions, 500 μg of *p*-nitrophenyl β-D-glucuronide (PNP-GLC) was completely hydrolyzed (data not shown).

The polar residues were analyzed before and after enzymatic treatment by HPLC (C18HPLC Method 4) with a C18 column with the following conditions: solvent A = water with 5 mM NH_4Ac (not pH-adjusted), solvent B = methanol with 5 mM NH_4Ac; flow rate = 1 mL/min; gradient for 0−10 min = 60% B, for 10−50 min = 60−100% B, and for 50−60 min = 100% B.

HPLC Analysis of DMSO Extract. The DMSO extract of the M/W marc from composited RAC of the 5× plants (3 days PHI) was dried under a heat lamp, and the residue was dissolved in methanol and assayed by C18HPLC Method 1.

HPLC Analysis of Glucose and Derivatives. [^{14}C]-Glucose and the radioactivity in the supernatant after addition of [^{14}C]glucose to and acid hydrolysis of the DMSO marc from RAC of control plants were analyzed by CHOHPLC. An IBM carbohydrate column was eluted with acetonitrile (Solvent A) and water (Solvent B) at a flow rate of 1 mL/min with the following gradient: 0−30 min = 20% B, 20−25 min = 25−100% B, 25−50 min = 100% B. The phenylosazones obtained from phenylhydrazine derivatization of the acid hydrolysate of the DMSO marcs from RAC of control and treated plants were analyzed by C18HPLC Method 5. An Axxiom C18 column was eluted with 5 mM NH_4Ac in methanol (solvent B) and 5 mM NH_4Ac in water (solvent A) at a flow rate of 1 mL/min, with the following gradients: 0−20 min = 65% B, 20−25 min = 25−100% B, 25−50 min = 100% B. The eluate was monitored at 254 nm, and 1-min fractions were collected for LSC assay.

RESULTS

Plant Condition during Harvest. There appeared to be a trend for a consistent increase in total leaf mass with time of harvest in the 5× plants but no trend was seen in the 1× plants (Figure 5). The head leaf was always the largest leaf fraction, followed by wrapper leaf and dead leaf, and there appeared to be no significant changes in the relative proportions of these leaf fractions during harvest for both treatment groups (Figure 5). The plants were of comparable quality to the commercial product.

Table 1. Percent Distribution of Total Residue in Lettuce Plants[a]

		dead leaf		RAC		root	
PHI		mean, %	SD, %	mean, %	SD, %	mean, %	SD, %
(1×)							
2 h	^{14}C	0.37	5.03	79.43	5.08	0.19	0.07
	^{3}H	*0.58*	*0.40*	*99.42*	*0.40*	*0*	
1 day	^{14}C	47.58	4.12	52.31	4.10	0.12	0.06
	^{3}H	*14.24*	*6.48*	*85.76*	*6.48*	*0*	
3 days	^{14}C	57.38	18.56	42.19	18.67	0.43	0.20
	^{3}H	*25.48*	*22.34*	*74.52*	*22.34*	*0*	
7 days	^{14}C	46.45	17.79	53.31	17.90	0.24	0.14
	^{3}H	*15.83*	*10.37*	*84.17*	*10.37*	*0*	
10 days	^{14}C	73.40	6.09	25.95	6.05	0.65	0.10
	^{3}H	*61.57*	*1.99*	*38.43*	*1.99*	*0*	
(5×)							
2 h	^{14}C	25.47	4.32	74.28	4.27	0.24	0.09
	^{3}H	*7.70*	*12.18*	*92.30*	*12.18*	*0*	
1 day	^{14}C	32.21	25.42	67.66	25.42	0.14	0.02
	^{3}H	*13.46*	*20.12*	*86.54*	*20.12*	*0*	
3 days	^{14}C	42.14	20.24	57.50	20.25	0.36	0.04
	^{3}H	*16.28*	*13.37*	*83.72*	*13.36*	*0*	
7 days	^{14}C	60.16	13.27	39.53	13.30	0.30	0.05
	^{3}H	*46.90*	*17.11*	*53.10*	*17.10*	*0*	
10 days	^{14}C	47.56	15.64	51.81	15.79	0.62	0.18
	^{3}H	*22.50*	*4.27*	*77.50*	*4.27*	*0*	

[a] Mean and standard deviation percent of total ^{14}C-residue and ^{3}H-residue in dead leaf, RAC, and root for three plants per PHI and rate.

Table 2. Concentration of Total ^{14}C-Residue in Lettuce RAC[a]

	1×		5×	
PHI	mean, ppb	SD, ppb	mean, ppb	SD, ppb
2 h	365	89	1614	164
1 day	312	86	1543	811
3 days	193	59	940	349
7 days	193	59	599	262
10 days	81	22	619	207

[a] Mean and standard deviation of total ^{14}C-residue in lettuce RAC for three plants per rate and PHI expressed as ppb MAB1A benzoate equivalents.

Distribution and Concentration of Total Residue in Lettuce Plants. The portion of total plant ^{14}C-labeled residue (^{14}C-residue) in the RAC of 1× and 5× plants declined from ~75−80% at 2 h PHI to ~25−50% after 10 days. There was a concomitant increase in the dead leaf ^{14}C-residue from ~20−25% of the total plant residue at 2 h to ~50−75% at 10 days (Table 1). The portion of total plant ^{14}C-residue in the root of 1× and 5× plants appeared to increase from ~0.2% at 2 h to ~0.6% at 10 days (Table 1). The portion of total plant ^{3}H-labelled residue (^{3}H-residue) in the RAC of 1× and 5× plants declined from ~90−99% at 2 h PHI to ~40−80% after 10 days. There was a concomitant increase in the dead leaf ^{3}H-residue from ~1−10% of the total plant ^{3}H-residue at 2 h to ~20−60% at 10 days (Table 1). No ^{3}H-residue was detected in roots.

The total ^{14}C-residue (expressed as MAB1A benzoate equivalents) of the RAC declined from 365 ppb at 2 h PHI to 81 ppb by 10 days for the 1× plants and from 1616 to 619 ppb for the 5× plants over the same interval (Table 2).

Effect of Methanol Rinsing on Total ^{14}C-Residue in RAC Leaf Fractions. In general, when the contri-

Table 3. Effect of Methanol Rinsing on ^{14}C-Residue in Head and Wrapper Leaf[a]

	head					wrapper				
	LR		RL			LR		RL		
PHI	mean	SD	mean	SD	total	mean	SD	mean	SD	total
(1×)										
2 h	4.5	4.4	2.4	1.3	6.8	59.3	2.3	33.9	3.3	93.2
1 day	6.5	8.4	3.4	3.5	9.9	56.9	10.9	33.2	0.9	90.1
3 days	6.8	5.5	6.0	2.8	12.8	44.8	5.5	42.4	9.8	87.2
7 days	3.9	2.2	4.6	1.8	8.6	40.1	3.5	51.3	3.5	91.4
10 days	5.2	3.6	9.3	1.1	14.5	45.6	3.3	40.0	7.0	85.5
(5×)										
2 h	6.1	4.5	2.9	1.1	9.0	63.3	4.2	27.6	3.4	91.0
1 day	22.3	28.3	2.1	1.2	24.5	48.7	39.2	26.8	10.5	75.5
3 days	4.1	2.5	3.4	0.5	7.5	61.3	8.0	31.2	6.5	92.5
7 days	4.2	1.9	6.3	2.7	10.5	51.6	7.9	37.9	3.9	89.5
10 days	1.9	0.7	4.8	1.5	6.7	51.1	7.4	42.2	6.8	93.3

[a] Normalized distribution (%) of total ^{14}C-residue of RAC among leaf fractions (head and wrapper leaf) after rinsing with methanol. Values determined by liquid scintillation counting (LSC) without combustion for all fractions. No significant difference was seen between direct LSC counting and radiocombustion analysis of rinsed leaf homogenates (data not shown). Values are mean and standard deviation (SD) for three plants per rate and PHI. LR, leaf rinse; RL, rinsed leaf.

Table 4. Extractable ^{14}C-Residue of Lettuce RAC[a]

	^{14}C-residue	
PHI	extracted, %	unextracted, %
(1×)		
2 h	88.5	11.5
1 day	84.1	15.9
3 days	75.8	24.2
7 days	75.1	24.9
10 days	74.5	25.5
(5×)		
2 h	88.3	11.7
1 day	87.4	12.6
3 days	85.0	15.0
7 days	78.6	21.4
10 days	77.2	22.8

[a] The percent of total recovered carbon-14 radioactivity that was extractable by methanol/water for composited samples of three plants per rate and PHI. Recovery of radioactivity from the extraction of the RACs ranged from 100 to 110%.

bution of the leaf rinse and rinsed leaf were summed for each fraction, ~90% of the total ^{14}C-residue in the RAC of the 1× and 5× plants was in the wrapper leaf fraction and only ~10% was in the head leaf fraction (Table 3). There was a slight trend for an increase in the proportion of total ^{14}C-residue that remained in each leaf type after rinsing with increasing PHI (Table 3).

Fractionation of ^{14}C-Residue in Lettuce RAC by Sequential M/W Extraction, DMSO Extraction, and Acid Hydrolysis. The extractability of the total ^{14}C-residue of the RAC from the 1× and 5× plants by M/W declined somewhat with increasing PHI, from ~90% at 2 h to ~75% by 10 days (Table 4). In a separate experiment, the composited RAC (three plants each) from 5× plants (days 3 and 7 PHI) was successively extracted with the indicated percent of total ^{14}C-residue removed at each step: M/W (~80–85%), hot DMSO (~7%), and then was hydrolyzed with acid (~5–9%) leaving the final marc (~5%); (Table 5). The acid hydrolysis performed on the DMSO marc from the RAC of 5× plants (that remaining after M/W and DMSO extraction) gave somewhat variable results in replicate experiments (3 days PHI), where ~45% or 65% of the total carbon-14 radioactivity was released; however, ~65% of the carbon-14 radioactivity was also released from the DMSO marc from 7 days PHI plants (Table 5). Furthermore, when [^{14}C]glucose was added to DMSO marc from untreated plants prior to acid hydrolysis, a variable amount of radioactivity (~20% or 50%) was observed to associate with the final marc in replicate experiments (Table 5).

The supernatants (acid hydrolysates) after acid hydrolysis of the DMSO marcs from composited days 3 or 7 PHI 5× plants or from DMSO marcs from untreated (control) plants to which [^{14}C]glucose was added were derivatized with phenylhydrazine. In general, only a fraction (~15–60%) of the carbon-14 radioactivity, whether incurred or added exogenously as [^{14}C]glucose, was recovered as [^{14}C]phenylosazones (Table 5). A higher [^{14}C]phenylosazone yield was seen when [^{14}C]-glucose was added after (~40%) acid hydrolysis of DMSO marc from control plants rather than before (~15%); also, the [^{14}C]phenylosazone yields from the 5× plants (~20–60%) were comparable to those seen when [^{14}C]glucose was added exogenously to DMSO marc from untreated plants (Table 5).

HPLC and Quantitation of Extractable Residue Components. The resolution of eight avermectin standards by C18HPLC method 1 was at baseline with the exception of the 8AOXO-MAB1A and 8AOH-MAB1A compounds, which were partially resolved (Figure 6). The MFB1A compound apparently exists as a pair of relatively stable rotamers that were resolved by C18HPLC method 1 (Figure 6). The 15OH-MAB1A compound coeluted with the main rotamer of MFB1A by C18HPLC method 1 (data not shown). The tritium and carbon-14 radioprofiles of the extractable residue from the RAC of a 5× plant (2 h PHI) assayed by C18HPLC method 1 are shown in Figure 7. The carbon-14 radioprofile was at a higher but constant proportion to that of the tritium radioprofile at the elution time of the peak corresponding to the main rotamer of MFB1A plus 15OH-MAB1A and beyond; however, for the radioactivity eluting before that peak, the carbon-14 radioprofile became increasingly greater than the tritium radioprofile as elution time decreased (Figure 7). In general, the quantitative contribution of each component to the total extractable ^{14}C-residue was remarkably similar between the 1× and 5× rates (Table 6). The major component of the extractable ^{14}C-residue at all PHIs was the polar residues, which increased from ~30% at 2 h PHI to ~75% by 10 days (Table 6). The parent MAB1A rapidly decreased, from ~30% of the total extractable ^{14}C-residue at 2 h PHI to only ~4% by 10 days (Table 6). The residue components coeluting with standards that are derivatives with one structural change relative to MAB1A (MSB1A, FAB1A, 15OH-

Table 5. Sequential Fractionation of RAC from 5× Plants[a]

RAC fraction	PHI 3 days (% STEP)	PHI 3 days (% RAC)	PHI 7 days (% STEP)	PHI 7 days (% RAC)	control (% STEP)
RAC	*100*	*100*	*100*	*100*	
methanol/water extract (A)	84.15	**84.15**	78.51	**78.51**	
methanol/water marc	15.85	15.85	21.49	21.49	
methanol/water marc	*100*	*15.85*	*100*	*21.49*	
DMSO extract (A)	41.09	**6.51**	33.09	**7.11**	
DMSO marc	58.91	9.34	66.91	14.38	
DMSO marc	*100*	*9.34*	*100*	*14.38*	*100*
acid hydrolysate, replicate 1	64.69	6.04	63.63	9.15	80.80
acid hydrolysate, replicate 2	45.60	4.26			51.30
acid hydrolysate, mean	55.15	5.15	63.63	9.15	66.05
final marc, replicate 1	35.31	3.30	36.37	5.23	19.20
final marc, replicate 2	54.40	5.08			48.70
final marc, mean (A)	44.86	**4.19**	36.37	**5.23**	33.95
acid hydrolysate	*100*	*5.15*	*100*	*9.15*	*100*
derivatized, assay 1 (A)	22.1	**1.14**	60.20	**5.51**	14.65 (**B**)
underivatized, assay 1 (A)	77.9	**4.01**	39.80	**3.64**	85.35 (**B**)
derivatized, assay 2					38.70 (**C**)
underivatized, assay 2					61.30 (**C**)
total		**100**		**100**	

[a] Sequential extractions, acid hydrolysis, and derivatization of acid hydrolysate with phenylhydrazine for ^{14}C-residue from RAC of composited 5× plants (three plants per PHI) and derivatization of ^{14}C-glucose added to DMSO marc of untreated controls. All values are normalized to recovery in each step. Recoveries ranged from 77 to 107%. (**A**) Fractions in bold used for summation of total residue; (**B**) mean value of duplicate assays where [^{14}C]glucose was added to DMSO marc from control plants before acid hydrolysis; (**C**) [^{14}C]glucose was added to DMSO marc from control plants after acid hydrolysis.

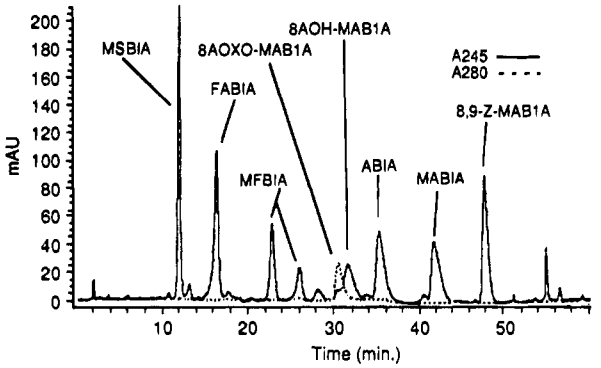

Figure 6. HPLC of avermectin standards. The UV profiles (245 and 280 nm) of reference standards chromatographed by C18HPLC method 1. MSB1A = avermectin B_{1a} monosaccharide; FAB1A = 4″-deoxy-4″-*epi*-(*N*-formyl)avermectin B_{1a}; MFB1A (rotamer pair) = 4″-deoxy-4″-*epi*-(*N*-formyl-*N*-methyl)-avermectin B_{1a}; 8AOXO-MAB1A = 8a-oxo-4″-deoxy-4″-*epi*-(methylamino)avermectin B_{1a}; 8AOH-MAB1A = 8a-hydroxydeoxy-4″-*epi*-(methylamino)avermectin B_{1a}; AB1A = 4″-deoxy-4″-*epi*-aminoavermectin B_{1a}; MAB1A = 4″-deoxy-4″-*epi*-(methylamino)avermectin B_{1a}; 8,9-*Z*-MAB1A = 8,9-*Z*-4″-deoxy-4″-*epi*-(methylamino)avermectin B_{1a}. The 15OH-MAB1A (14-exomethylene-15-hydroxy-4″-deoxy-4″-*epi*-(methylamino)avermectin B_{1a}) standard coelutes with the main rotamer of MFB1A (not shown).

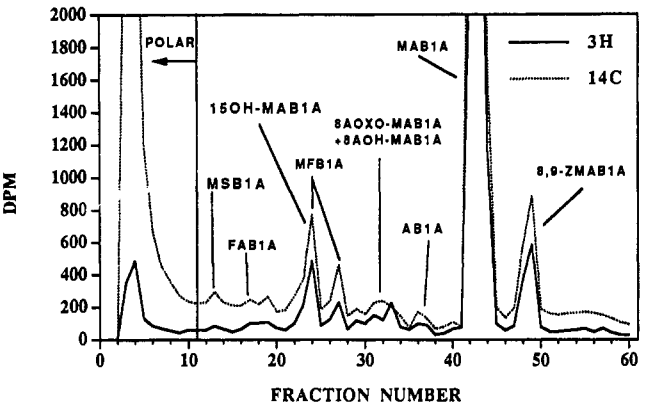

Figure 7. HPLC assay of extractable residue from lettuce RAC. The extractable residue from the RAC of an individual plant from the 5× plot (2 h PHI) was assayed by C18HPLC method 1. Polar residues indicated as all radioactivity eluting before MSB1A. Abbreviations for standards indicated that coelute with radioactivity peaks are given in Figure 6 and in main text.

MAB1A+MFB1A, 8AOXO- + 8AOH-MAB1A, AB1A, 8,9-Z-MAB1A) in general remained fairly constant from 2 h to 3 days PHI and then decreased thereafter (Table 6). No residue component except MAB1A and the polar residues contributed to more than 10% of the total extractable ^{14}C-residue at any time except for MFB1A+15OH-MAB1A (13.8%) in the 1× plants at 2 h PHI (Table 6). As with the extractable ^{14}C-residue (Table 6), in general, the quantitative contribution of each component to the total extractable ^{3}H-residue was remarkably similar between the 1× and 5× rates (Table 7). The major component of the extractable ^{3}H-residue at all PHIs except at 2 h was the polar residues, which increased from ~10% at 2 h PHI to ~60−70% by 10 days (Table 7). The parent MAB1A, which was only ~50% of the total extractable ^{3}H-residue at 2 h PHI, continued this rapid decrease to only ~4% of the total extractable ^{3}H-residue by 10 days (Table 7). The residue components coeluting with standards with one structural change relative to MAB1A (MSB1A, FAB1A, 15OH-MAB1A+MFB1A, 8AOXO- + 8AOH-MAB1A, AB1A, 8,9-Z-MAB1A) in general remained fairly constant from 2 h to 3 days PHI and then decreased thereafter, with the exception of MSB1A and FAB1A, which did not decrease until 10 days PHI (Table 7). No residue component except MAB1A and the polar residues contributed to more than 10% of the total extractable ^{3}H-residue at any time except for MFB1A+15OH-MAB1A in the 1× plants at 2 h and 1 day PHI (Table 7). The parent MAB1A rapidly declined in lettuce RAC from ~100 (1×) or 500 (5×) ppb (expressed as MAB1A benzoate equivalents) at 2 h PHI to only ~2 (1×) or 20 (5×) ppb by 10 days (Figure 8). The polar residues in lettuce RAC increased from ~100 (1×) or 500 (5×) ppb (expressed as MAB1A benzoate equivalents) at 2 h PHI to ~120 (1×) or 600 (5×) ppb at 1 day PHI, then declined to ~40 (1×) or 350 (5×) ppb by 10 days (Figure 8).

Components of the extractable residue from composited RAC of 5× plants (3 days PHI) were identified after

Table 6. HPLC Assay of Extractable ^{14}C-Residue from RAC of Individual Plants[a]

	eluted radioactivity, %									
	2 h PHI		1 day PHI		3 days PHI		7 days PHI		10 days PHI	
residue	1×	5×	1×	5×	1×	5×	1×	5×	1×	5×
polar	**28.9**	**36.5**	**46.7**	**45.7**	**60.9**	**57.9**	**75.2**	**68.7**	**77.5**	**74.6**
	4.9	*3.3*	*4.6*	*13.5*	*1.9*	*9.0*	*1.3*	*1.7*	*3.2*	*1.5*
MSB1A	**2.9**	**1.7**	**3.2**	**2.6**	**3.8**	**2.5**	**2.7**	**2.4**	**0.7**	**2.0**
	0.3	*0.1*	*0.3*	*0.2*	*0.1*	*0.1*	*0.1*	*0.3*	*0.1*	*0.3*
FAB1A	**2.8**	**2.2**	**2.8**	**3.5**	**2.5**	**3.0**	**2.1**	**2.1**	**1.5**	**1.5**
	0.3	*0.3*	*0.4*	*0.4*	*0.6*	*0.4*	*0.4*	*0.4*	*0.8*	*0.2*
MFB1A+150H-MAB1A	**13.8**	**6.5**	**7.5**	**6.7**	**5.1**	**5.5**	**3.2**	**3.4**	**1.9**	**2.4**
	1.5	*0.6*	*1.1*	*1.5*	*0.7*	*1.3*	*0.2*	*0.1*	*0.3*	*0.3*
8AOXO-MAB1A+8AOH-MAB1A	**3.4**	**3.0**	**2.9**	**3.7**	**1.9**	**2.8**	**1.2**	**2.4**	**1.1**	**1.8**
	0.3	*0.8*	*0.6*	*0.8*	*0.5*	*1.1*	*0.4*	*0.6*	*0.6*	*0.2*
AB1A	**1.6**	**1.1**	**1.3**	**1.3**	**0.8**	**0.9**	**0.5**	**0.7**	**0.7**	**0.6**
	0.2	*0.1*	*0.0*	*0.5*	*0.0*	*0.4*	*0.1*	*0.2*	*0.2*	*0.1*
MAB1A	**30.5**	**32.4**	**18.1**	**17.1**	**9.3**	**11.1**	**4.7**	**7.3**	**3.5**	**4.1**
	3.8	*3.3*	*2.9*	*6.6*	*1.5*	*3.8*	*0.4*	*1.2*	*0.3*	*0.7*
8,9-*Z*-MAB1A	**4.9**	**4.7**	**4.1**	**4.4**	**2.6**	**2.8**	**1.7**	**1.6**	**1.5**	**1.4**
	0.6	*0.5*	*0.6*	*1.6*	*0.2*	*1.4*	*0.1*	*0.6*	*0.4*	*0.2*
undefined	**11.2**	**11.9**	**13.4**	**15.0**	**13.0**	**13.7**	**8.6**	**11.6**	**11.7**	**11.5**
	0.7	*0.5*	*0.4*	*2.3*	*1.8*	*0.6*	*0.3*	*0.7*	*1.5*	*1.0*
total	100	100	100	100	100	100	100	100	100	100

a The methanol/water-extractable ^{14}C-residue of the RAC from all individual treated plants was assayed by C18HPLC Method 1. Values are mean (bold) and standard deviation (italics) of the percent of eluted radioactivity corresponding to the indicated added standards, corresponding to that eluting before the MSB1A standard (designated "polar"), or corresponding to the total not accounted for by co-elution with standards and eluting after the MSB1A standard (designated "undefined"); see Figure 7. The extractable ^{14}C-residue ranged from 74 to 89% of the total ^{14}C-residue (Table 4).

Table 7. HPLC Assay of Extractable ^{3}H-Residue from RAC of Individual Plants[a]

	eluted radioactivity, %									
	2 h PHI		1 day PHI		3 days PHI		7 days PHI		10 days PHI	
residue	1×	5×	1×	5×	1×	5×	1×	5×	1×	5×
polar	**8.6**	**10.0**	**25.3**	**30.3**	**51.2**	**42.6**	**67.0**	**71.1**	**62.1**	**71.8**
	1.3	*0.2*	*4.4*	*13.6*	*0.6*	*12.5*	*0.4*	*7.8*	*27.8*	*3.4*
MSB1A	**2.0**	**1.2**	**3.4**	**2.6**	**4.1**	**2.7**	**3.2**	**2.9**	**0.7**	**2.8**
	0.3	*0.2*	*0.4*	*0.3*	*0.2*	*0.2*	*0.1*	*0.5*	*0.8*	*0.2*
FAB1A	**2.8**	**2.0**	**3.3**	**4.2**	**3.3**	**4.2**	**3.0**	**2.2**	**0.8**	**1.9**
	0.5	*0.2*	*0.2*	*0.5*	*0.8*	*0.4*	*0.3*	*0.5*	*1.3*	*0.3*
MFB1A+150H-MAB1A	**18.7**	**8.6**	**11.9**	**8.6**	**6.5**	**7.8**	**4.9**	**3.1**	**2.9**	**2.8**
	1.8	*1.7*	*0.7*	*1.5*	*1.1*	*1.3*	*0.8*	*1.7*	*2.5*	*0.7*
8AOXO-MAB1A+8AOH-MAB1A	**4.0**	**3.9**	**4.3**	**5.1**	**2.9**	**3.9**	**1.8**	**2.5**	**1.3**	**2.4**
	0.5	*0.6*	*1.0*	*1.1*	*1.2*	*1.3*	*0.2*	*1.4*	*1.7*	*0.3*
AB1A	**2.0**	**1.8**	**1.4**	**1.6**	**1.7**	**1.9**	**0.6**	**0.1**	**0.5**	**0.4**
	0.2	*0.1*	*0.9*	*0.6*	*0.4*	*1.0*	*0.5*	*0.2*	*0.5*	*0.1*
MAB1A	**45.6**	**54.5**	**29.7**	**25.5**	**12.4**	**15.9**	**7.1**	**7.7**	**2.5**	**4.8**
	4.6	*1.3*	*2.8*	*2.9*	*1.7*	*8.1*	*0.9*	*0.4*	*1.6*	*1.2*
8,9-*Z*-MAB1A	**6.3**	**6.7**	**6.0**	**5.7**	**2.4**	**3.9**	**2.0**	**1.5**	**0.8**	**1.4**
	0.6	*0.8*	*0.8*	*2.1*	*0.2*	*2.2*	*0.1*	*0.6*	*0.7*	*0.2*
undefined	**9.9**	**11.3**	**14.7**	**16.4**	**15.5**	**16.9**	**10.4**	**9.0**	**28.4**	**11.7**
	0.9	*1.0*	*1.8*	*0.9*	*2.2*	*3.4*	*1.4*	*4.3*	*25.7*	*1.7*
total	**100**	**100**	**100**	**100**	**100**	**100**	**100**	**100**	**100**	**100**

a The methanol/water-extractable ^{3}H-residue of the RAC from all individual treated plants was assayed by C18HPLC Method 1. Values are mean (bold) and standard deviation (italics) of the percent of eluted radioactivity corresponding to the indicated added standards, corresponding to that eluting before the MSB1A standard (designated "polar"), or corresponding to the total not accounted for by co-elution with standards and eluting after the MSB1A standard (designated "undefined"; see Figure 7.

first chromatographing the extractable residue with standards by C18HPLC Method 1 (Figure 9A) and then rechromatographing the pooled eluate fractions corresponding to the standards by CATHPLC or SIHPLC (Figure 9B–H). When rechromatographed, the MSB1A fractions (Figure 9B) contained multiple residues, with MSB1A accounting for only a small fraction of the radioactivity. After rechromatography, the FAB1A fraction contained FAB1A as the major constituent, but other minor residues were apparent (Figure 9C). The rechromatography of the MFB1A+15OH-MAB1A fractions (Figure 9D) resolved these compounds. The fractions containing unresolved 8AOXO-MAB1A and 8AOH-MAB1A residues were separated by the second chromatography into approximately equal proportions of the two compounds with no other residue components apparent (Figure 9E). The AB1A fractions were resolved (Figure 9F) into three major components (AB1A, X1, X2), with AB1A accounting for only a minor portion of the total radioactivity. The parent MAB1A was essentially the only constituent in the MAB1A fractions (Figure 9G). Finally, the 8,9-Z-MAB1A fractions contained 8,9-Z-MAB1A as the major constituent, but two minor unknown residues (Y1, Y2) were also observed (Figure 9C–E,G,H).

An attempt was also made to resolve the polar extractable residues by serial HPLC. The polar residues were obtained from the extractable residue of the composited RAC from 5× plants (3 days PHI) by C18HPLC Method 2 (not shown) and then chromatographed by C18HPLC Method 3 (Figure 10A), which resulted in a sharp peak of unretained radioactivity and

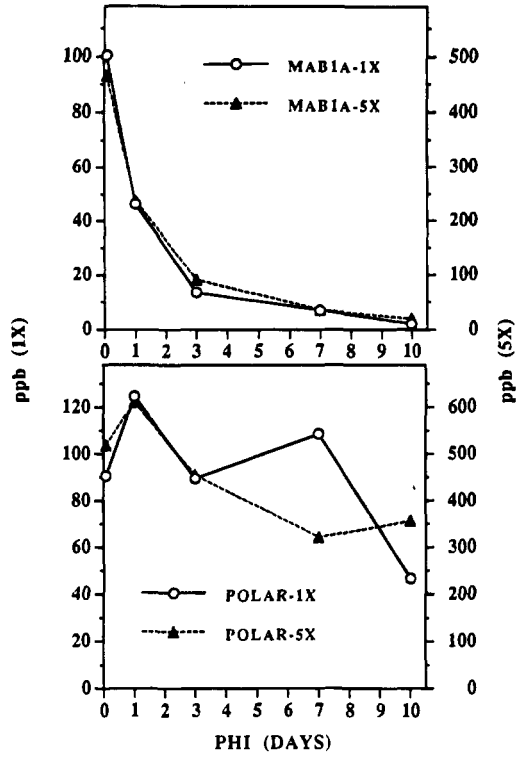

Figure 8. MAB1A and polar residue levels in lettuce RAC. The extractable ^{14}C-residue from the RAC of the 1× and 5× plants was assayed by C18HPLC Method 1, and the levels of the polar residues and MAB1A were expressed as MAB1A benzoate equivalents. Values are means from three plants per PHI and rate.

a broad composite of unresolved peaks of retained radioactivity eluting over the entire gradient. When 10 sets of sequentially pooled fractions of eluate (each representing ~10% of the total eluted carbon-14 radioactivity) were assayed by DIOLHPLC, no significant resolution of major components was seen, rather unresolved or multiple minor components were noted (Figure 10A–J). This DIOLHPLC method contained both acidic (acetate) and basic (TEA) modifiers and sharp, well resolved peaks were obtained when MAB1A and *p*-nitrophenol glucuronide were chromatographed (not shown), so it would be expected that residues containing acidic or basic functionalities would not broaden due to secondary interactions with the column. Also, this DIOLHPLC method employed a gradient where the eluent polarity ranges from relatively nonpolar (1 methylene chloride:2 hexane) to polar (methanol) over 60 min; therefore, any broad peaks observed are likely to consist of multiple components. The sharp, unretained peak of radioactivity (Figure 10A) appeared as multiple components when rechromatographed (Figure 10A, inset). The relative retention order of the 10 sets of polar residue fractions by C18HPLC Method 3 (Figure 10A) was roughly reversed as expected in the DIOLHPLC method (Figure 10A–J).

Enzymatic Treatments of Polar Extractable Residue. Treatment of the polar extractable residues with α- or β-glucosidase or β-glucuronidase did not result in release of conjugated avermectin-like residues. Analysis by HPLC method 5 before and after the enzymolyses resulted in an unretained peak of radioactivity eluting before the MSB1A standard while all other avermectin standards including MAB1A eluted after MSB1A (data not shown). Acid hydrolyis of polar residues was attempted with 0.2 M HCl, but no release of conjugates was observed (data not shown). Concentrations of HCl

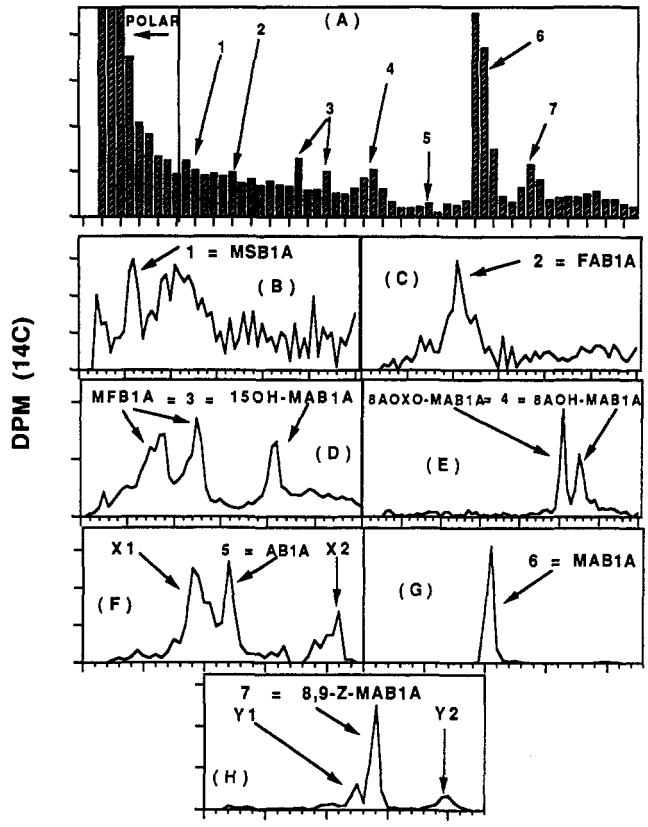

Figure 9. Identification of extractable residue components. The extractable residue from composited lettuce RAC (5×, 3 days PHI) and a mixture of standards were cochromatographed by C18HPLC Method 1. Fractions corresponding to UV peaks of standards were rechromatographed by SIHPLC or CATHPLC: (**A**) radioprofile of extractable residue with radioactivity peaks 1–7 corresponding to UV peaks (not shown) of added standards; (**B**–**H**) radioprofiles after SIHPLC (**B**, **C**, **D**, **E**) or CATHPLC (**F**, **G**, **H**) of residue components indicated in (**A**) with radioactivity peaks corresponding to UV peaks (not shown) of indicated standards. The peaks X1, X2, Y1, Y2 are unknowns.

equal to or exceeding 0.5 M HCl rapidly degraded MAB1A to polar compounds (data not shown) so that treatment of polar residues under these conditions would result in no observable MAB1A release.

HPLC Analysis of DMSO Extract. When the DMSO extract of the M/W marc from composited RAC from 5× plants (3 days PHI) was dried under a heat lamp and reconstituted in methanol, ~60% of the carbon-14 radioactivity was solubilized. When MAB1A was heated at 80 °C overnight in DMSO, no degradation occurred, and only partial degradation was seen when this DMSO solution was dried under a heat lamp and reconstituted in methanol (data not shown). The analysis of the methanol-soluble fraction of this reconstituted DMSO extract from the plants resulted in a peak of unretained radioactivity eluting before MSB1A when assayed by C18HPLC method 1 (data not shown).

HPLC Analysis of Glucose and Derivatives. HPLC analysis of the soluble radioactivity after acid treatment of DMSO marc from untreated plants to which [^{14}C]glucose was added indicated that severe degradation of glucose had occurred (Figure 11). HPLC analysis of the [^{14}C]phenylosazone derivatives of the radioactivity released by acid hydrolysis of DMSO marc from 5× plants or those of the radioactivity after acid treatment of DMSO marc from untreated plants to which [^{14}C]glucose was added indicated that at least two types of derivatives had formed and that these deriva-

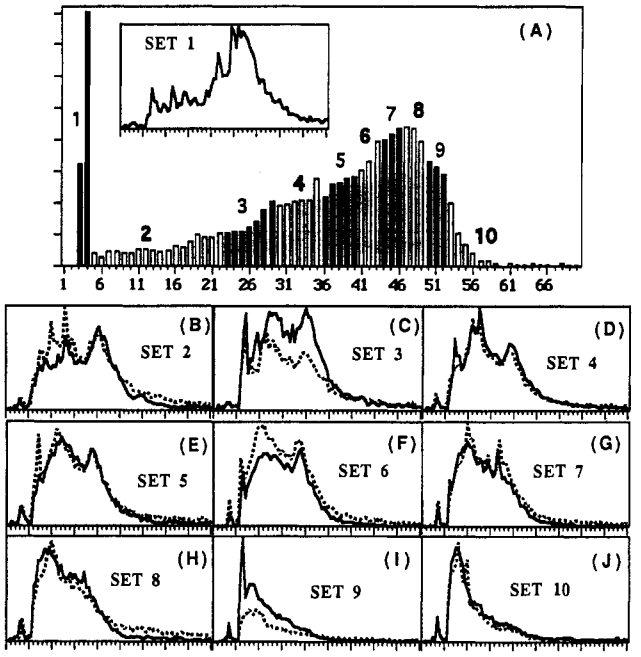

Figure 10. HPLC characterization of polar extractable residue. The polar extractable residue was obtained from the extractable residue from composited RAC of 5× plants (3 days PHI) by C18HPLC Method 2. The residue was then rechromatographed by C18HPLC method 3. Ten sets of eluate fractions were obtained, and each was then rechromatographed by DIOLHPLC: (**A**) radioprofile (^{14}C) of polar extractable residue from C18HPLC method 3 and 10 sets of pooled eluate fractions (inset, Set 1 assayed by DIOLHPLC); (**B**–**J**) radioprofiles (^{14}C) of Sets 2–10 assayed by DIOLHPLC. The procedure was repeated, and for Sets 2–10 (**B**–**J**), the two profiles indicated are the replicate assays. Set 1 was not assayed in replicate.

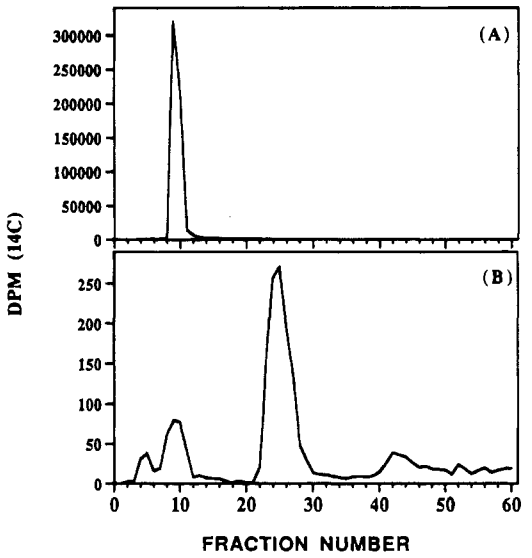

Figure 11. HPLC analysis of [^{14}C]glucose before and after acid treatment of DMSO marc. Glucose (^{14}C) was added to DMSO marc from RAC of untreated plants prior to acid treatment, and the supernatant was analyzed by CHOHPLC after hydrolysis: (**A**) glucose before acid treatment; (**B**) supernatant after acid hydrolysis.

tives were similar whether glucose was added to the marc or released from it (Figure 12).

DISCUSSION

The complex structure of MAB1A, its documented susceptibility to light-induced reactions (Feely et al., 1992), and the very low application rates for emamectin benzoate (0.015 lb of ai/acre maximum) assure that investigations of the nature of the residue in crops will be quite challenging, even before consideration of any metabolism that may occur in addition to photodegradation. The photodegradation of MAB1A as a thin film on glass results in at least nine primary (one change relative to MAB1A) and two secondary (two changes relative to MAB1A) photodegradates (Feely et al., 1992; Arison, 1991). The nature of the primary phototransformations includes *cis*–*trans* isomerization at the 8,9 position of MAB1A and two of its primary degradates, two oxidations at the 8a position (keto, hydroxy), oxidation at the 15 position (hydroxy), *N*-demethylation, oxidation (to *N*-formyl), or *N*-formylation at the 4″-*N*-methyl group, loss of the outer oleandrose sugar, and a double bond shift from the 3,4 to the 2,3 position. All of these thin film photodegradates, with the exceptions of the alkene 3,4 to 2,3 rearrangement and the 8,9-*Z*-photoisomers of two primary degradates, have been found at low levels as MAB1A residues in lettuce in the present study (Figure 4). The appearance of most of the same MAB1A photodegradates and photooxidation products as components of the residue in MAB1A-treated lettuce therefore suggests a nonmetabolic route. Further, it is apparent that the primary MAB1A degradates observed as a result of photolysis on glass or in lettuce are capable of undergoing additional reactions to a number of secondary, tertiary, or higher products as the demonstrated reactions alone can occur as 1–3 reaction types at five different sites in the molecule (4′, 4″, 8-9, 8a, and 15). For example, the 8,9-*Z*-isomers of the primary MAB1A degradates FAB1A and AB1A (8,9-*Z*-FAB1A and 8,9-*Z*-AB1A) were found as secondary photoproducts in thin films (Feely et al., 1992) and, given that formation of the 8,9-*Z*-isomer of MAB1A occurs on lettuce, it is possible that any lettuce residue with the diene intact, such as MSB1A, FAB1A, MFB1A, 8AOXO-MAB1A, 8AOH-MAB1A, AB1A, and 15OH-MAB1A (Figure 4), will exist as a pair of geometric isomers at the 8,9 position. The 8,9-*Z*-photoisomer of any primary degradate of MAB1A in lettuce, however,

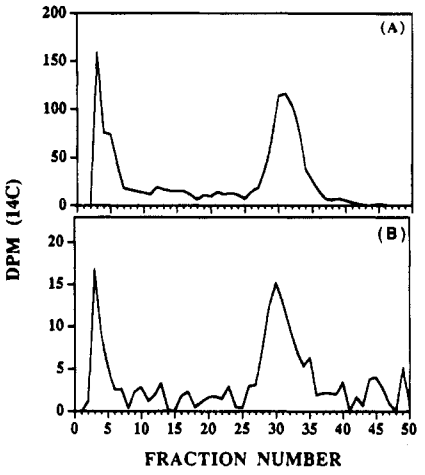

Figure 12. HPLC analysis of glucose phenylosazones. The phenylosazones obtained after derivatization of the acid hydrolysate of the DMSO marc from the RAC of composited 5× plants (3 days PHI) or the DMSO marc from untreated plants to which [^{14}C]glucose was added prior to hydrolysis were analyzed by C18HPLC method 5: (**A**) HPLC radioprofile of phenylosazones from acid hydrolysate of [^{14}C]glucose-added DMSO marc from untreated plants; (**B**) HPLC radioprofile of phenylosazones from acid hydrolysate of DMSO marc from treated plants.

would also be susceptible to photooxidative degradation and therefore would be found in extremely small amounts because no primary degradate contributes more than 10% to the total extractable residue at 1 day PHI or later (Table 6). The primary degradates of MAB1A observed in lettuce obviously are capable of additional light-catalyzed reactions other than photoisomerization at the 8,9 bond; for example the 4″-*N*-methyl of 15OH-MAB1A could be dealkylated, undergo *N*-formylation, or be oxidized to an *N*-formyl group, or the 8a position of 15OH-MAB1A could be oxidized to an alcohol or ketone; this would give a total of five additional potential degradates derived from 15OH-MAB1A, all of which, of course, could undergo photoisomerization at the 8,9 position. It is clear, then, that as long as MAB1A is exposed at the plant surface, a very large number of primary, secondary, and tertiary photodegradates would also be expected to be present.

This prediction of a large number of residue components resulting as end products of MAB1A photolysis in lettuce is apparent given the complexity observed for the polar extractable ^{14}C-residues from the RAC (Figure 10). The photodegradative pathway leading to these polar residues most likely includes other sites of reaction in the MAB1A molecule not discerned in this study or in previous work with MAB1A photolysis on glass (Feely et al., 1992). For example, cleavage at any number of C—O bonds such as between the inner oleandrose sugar and the macrocycle (C13), at the lactone (C19), the spiroketal (C17, C21, C25), or at the 8a carbon would result in a variety of potential degradates; and cleavage at any of the five double bonds by ketone, aldehyde, or carboxylate formation would also result in a number of potential degradates (Figure 1). These cleavages would be expected to produce more polar compounds. The various combinations possible with the known primary degradation reactions and the postulated C—O and C=C cleavages, therefore, could result in a very large number of compounds, such as oxygenated fragments of the macrocycle or ring-opened and oxygenated degradates of the macrocycle. Although little information is available regarding the end products of MAB1A photodegradation on glass, the very similar compound avermectin B_{1a} does photodegrade on glass to a complex, polar residue (Crouch et al., 1991) that is comparable to that found in avermectin B_{1a}-treated oranges (Crouch et al., 1992).

The structure of MAB1A presents a number of potential sites of metabolism by well-known enzymatic reactions, such as dealkylation, epoxidation, hydroxylation, ester or glycosidic hydrolysis, or *N*- or *O*-conjugation with sugars or glucuronic acid. The mammalian metabolism of several avermectins is well characterized. Avermectin B_{1a} (Maynard et al., 1989c, 1990), its 8,9-*Z*-photoisomer (Maynard et al., 1989b), and the 22,23-dihydro derivative of avermectin B_1, ivermectin (Chiu et al., 1987), for example, are metabolized in a number of species almost entirely to the 24-OH- and 3″-demethyl derivatives. A minor metabolite of ivermectin, a fatty acid ester of the 24-OH derivative, has been described in fat tissues of several species (Chiu et al., 1988). The metabolism of MAB1A has been examined in the rat (Mushtaq, personal communication) where only *N*-dealkylation to AB1A (Figure 4) occurs and to a minor degree. Thus, although the avermectin structure has a number of potential metabolic sites, the very active xenobiotic metabolism of mammals acts on a very limited number of these sites, with no major conjugates observed.

The fate of avermectins in plants with regard to metabolism by specific enzymes is unknown. Several previous studies of avermectin B_{1a} metabolism (Bull et al., 1984; Maynard et al., 1989a; Moye et al., 1990) found no metabolites corresponding to those found in mammals and the extractable residue consisted mostly of unknown polar degradates, avermectin B_{1a}, and its 8,9-*Z*-photoisomer. The unextractable residue of avermectin B_{1a}-treated celery, however, had ~5% of the total residue associated with lignin and ~5% of the total residue incorporated into glucose releasable by acid hydrolysis (Feely and Wislocki, 1991); the incorporation of residue into glucose is certainly indicative of the extensive degradation and fragmentation of the pesticide expected from photodegradation. It is possible, however, for a larger fragment of avermectin B_{1a} to first be cleaved to a smaller fragment of six carbons or less by plant enzymes prior to incorporation into glucose.

The occurrence of similar degradates of MAB1A in lettuce (Figure 4) and on glass (Feely et al., 1992; Arison, 1991) and the rapid rate of degradation of MAB1A in lettuce (Table 7) is far more consistent with photodegradation than metabolism in light of the limited metabolism of avermectins in mammals (Maynard et al., 1989b,c, 1990; Chiu et al., 1987) and in particular the limited metabolism of MAB1A in the rat (Mushtaq, personal communication) because the xenobiotic metabolism potential of animals is considered to be, in general, much greater than plants (Shimabukuro et al., 1988; Borlakoglu and John, 1989). Also, cytochrome P-450, known to be a route of oxidative metabolism in plants (Shimabukuro et al., 1988), appears to be absent in plant tissues where active photosynthesis occurs (Hendry, 1986), such as lettuce leaf. Further, the appearance of the MFB1A residue (Figure 4) as a major primary degradate (Figure 7; Tables 6 and 7) also strongly suggests photodegradation as the principle initial degradative route of MAB1A as this novel transformylation reaction is unlikely to be the result of metabolism; the 8,9-*Z*-MAB1A residue (Figure 4), another major primary degradate in lettuce (Figure 7; Tables 6 and 7) is also an unlikely metabolic product. In addition, the rapid breakdown of [^{3}H]MAB1A observed by 2 h PHI (Table 7) would almost certainly occur only on the leaf surface and therefore would be isolated from potential enzymatic attack as penetration into leaf cells would not be expected by that time. HPLC analysis of residues in wrapper leaf rinses and the extractable residue from rinsed wrapper leaf (data not shown) indicated that similar degradates were present. The residues in the methanol rinse were presumably removed from the cutin layer and not the cellular interior, so metabolism could not have resulted in the observed degradation. Finally, there was no apparent effect of application rate on the profile of degradates found in the extractable residue (Tables 6 and 7). It would be expected that if metabolism of MAB1A were the major route to these degradates, then the higher application rate would result in a slower rate of MAB1A breakdown.

The polar extractable ^{14}C-residue found in lettuce RAC could potentially contain products from conjugation reactions. The formation of *N*- and, more commonly, *O*-glycosides in plants is probably the predominant conjugative pathway in plants (Quistad and Menn, 1983). Analysis of the polar extractable ^{14}C-residue

after treatment with glucosidases and glucuronidase by HPLC, however, indicated that no sugar conjugates were present (data not shown). It is not known whether the polar extractable residues contain other conjugates of MAB1A or its degradates, such as those with amino acids or glutathione. However, neither MAB1A itself nor any of the identified residue components contains any reactive positions for conjugation with glutathione or amino acids. Further, any unknown MAB1A degradates with reactive positions capable of conjugation, if any, would be expected to be very minor.

The ^{14}C-residue in lettuce RAC unextractable by methanol and aqueous methanol (M/W extraction) were partially associated with lignin as indicated by extractability with hot DMSO; ~7% of the total ^{14}C-residue of the RAC was associated with this fraction (Table 5). However, any starch present also would have been extracted during this step and possibly other natural products. Whether the carbon-14 radioactivity extractable with hot DMSO represents incorporation into or association with lignin or other natural products was not addressed in the present study. The portion of the DMSO-extractable ^{14}C-residue soluble in methanol did not contain residue components corresponding to any of the reference standards used (Figure 4) when analyzed by HPLC (data not shown). Another portion of the unextractable ^{14}C-residue was incorporated into glucose, which was presumably released from cellulose and other polysaccharides after acid hydrolysis of the DMSO marc. The exact quantitation of incorporation into glucose, however, was compromised due to the apparent degradation of glucose during acid hydrolysis of the DMSO marc (Figure 11) and the lack of quantitative derivatization of glucose (Table 5). Nevertheless, because carbon-14 radioactivity from [^{14}C]glucose added exogenously prior to the acid hydrolysis of the DMSO marc from untreated plants was derivatized with phenylhydrazine to a similar extent as the carbon-14 radioactivity released from the DMSO marc of treated plants (Table 5) and because similar phenylosazones were formed (Figure 12), it can be assumed that much of the carbon-14 radioactivity in the acid hydrolysate of DMSO marc (~5–10% of the total RAC residue) came from cellulose and other polysaccharides (Table 5). The incorporation of ^{14}C-residue into glucose and association with DMSO-soluble lignin was previously observed in avermectin B_{1a}-treated celery (Feely and Wislocki, 1991). The incorporation of ^{14}C-residue into glucose obviously requires extensive degradation of the MAB1A molecule, but the source of the immediate precursors is not apparent nor would it be easily established. The fragmentation of the MAB1A molecule by photodegradative cleavage at ether linkages and double bonds as suggested may yield fragments of six carbons or less, but such a fragmentation retaining radiolabel is not readily apparent from the MAB1A structure (Figure 1). Because free glucose, other monosaccharides, and sucrose soluble in methanol would be expected to be found in the polar extractable residue fraction (Figures 2 and 7), it is likely that some of these polar ^{14}C-residues also represent incorporation into those sugars. However, this was not determined. The remaining bound ^{14}C-residue, ~5% of the total RAC ^{14}C-residue (Table 5), was not characterized further but likely represents incorporation into natural products.

The loss of ^{14}C-residue from lettuce RAC in both the 1× and 5× plants (Table 2) with increasing PHI (expressed as ppb MAB1A benzoate equivalents) did not appear to result from an increase in plant mass. Although an increase in mass did occur in the 5× plants over the entire PHI, none was observed in the 1× plants (Figure 5). Furthermore, because the plants were harvested at maturity during which significant increases in mass would not be expected, and because a significant decrease in residue and a decrease in mass was observed in the 5× plants between 3 and 7 days PHI (Table 2; Figure 5), then the apparent increase in 5× plant mass during harvest is probably due to chance variation in plant size and not growth. The loss of ^{14}C-residue from the RAC with increasing PHI (Table 2) did result in part from an increase in ^{14}C-residue in dead leaf (Table 1), although there was no trend for an increase in dead leaf mass with time (Table 5). This increase in the ^{14}C-residue of dead leaf with increasing PHI could be interpreted most simply if dead leaf increased with time but was also becoming desiccated, resulting in no apparent increase in mass. The loss of ^{14}C-residue from the RAC with increasing PHI (Table 2) could also partially result from the presumed extensive degradation of MAB1A into small molecules because this would be required for the observed incorporation of carbon-14 radioactivity into glucose and DMSO-soluble lignin (Table 5). Therefore, loss of radiolabel could occur due to the production of fragments that are volatile or that produce [^{14}C]CO_2 during metabolic turnover.

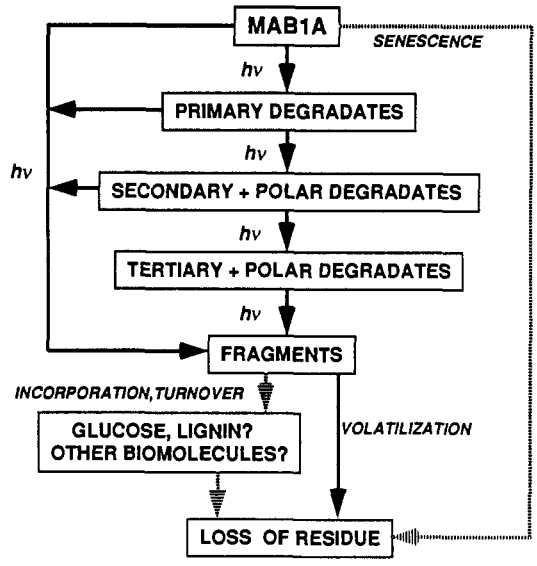

Figure 13. Proposed pathways for MAB1A degradation in lettuce RAC.

In summary (Figure 13), the fate of emamectin benzoate in lettuce appears to be an initial rapid breakdown by photodegradation and photooxidation to a number of primary products that in turn undergo additional sequential photoreactions to produce a complex residue of extremely numerous minor components. The fragmentation of the avermectin macrocycle in these emamectin degradates by photolytic and photooxidative processes and/or possibly by plant enzymes then results in partial incorporation into plant natural products.

ABBREVIATIONS USED

15OH-MAB1A, 14-exomethylene-15-hydroxy-4″-deoxy-4″-*epi*-(methylamino)avermectin B_{1a}; 8,9-*Z*-MAB1A, 8,9-*Z*-4″-deoxy-4″-*epi*-(methylamino)avermectin B_{1a}; 8AOH-MAB1A, 8a-hydroxy-4″-deoxy-4″-*epi*-(methylamino)-

avermectin B_{1a}; 8AOXO-MAB1A, 8a-oxo-4″-deoxy-4″-*epi*-(methylamino)avermectin B_{1a}; AB1A, 4″-deoxy-4″-*epi*-aminoavermectin B_{1a}; AGLU, α-glucosidase; ai, active ingredient; BGLC, β-glucuronidase; BGLU, β-glucosidase; C18HPLC, HPLC with a C18 column; CATHPLC, HPLC with a C8/cation-exchange column; CHOHPLC, HPLC with an IBM carbohydrate column; DIOLHPLC, HPLC with a diol column; DMSO, dimethyl sulfoxide; FAB1A, 4″-deoxy-4″-*epi*-(*N*-formyl)-avermectin B_{1a}; HPLC, high-pressure liquid chromatography; LSC, liquid-scintillation counting; M/W, methanol/water; MAB1, mixture of MAB1A and MAB1B avermectins in MK-0244; MAB1A, 4″-deoxy-4″-*epi*-(methylamino)avermectin B_{1a}; MAB1B, 4″-deoxy-4″-*epi*-(methylamino)avermectin B_{1b}; MFB1A, 4″-deoxy-4″-*epi*-(*N*-formyl-*N*-methyl)avermectin B_{1a}; MSB1A, avermectin B1a monosaccharide; PHI, preharvest interval; PNP-GLC, β-D-glucuronide; PNP-GLU, *p*-nitrophenyl, α-D-glucopyranoside; RAC, raw agricultural commodity; RCA, radiocombustion analysis; SIHPLC, HPLC with a silica column; NaAc; sodium acetate; TEA, triethylamine.

ACKNOWLEDGMENT

We thank Eric Feutz and Brian Jacobson of ABC Laboratories for their expert advice, the contribution of their considerable horticultural talents, and their assistance with sample preparation.

LITERATURE CITED

Arison, B. H. Merck Research Laboratories, personal communication, 1991.

Borlakoglu, J. T.; John, P. Cytochrome P-450 metabolism of xenobiotics. A comparative study of rat hepatic and plant metabolism. *Comp. Biochem. Physiol.* **1989**, *94C*, 613–617.

Bull, D. L.; Ivie, G. W.; MacConnell, J. G.; Gruber, V. F.; Ku, C. K.; Arison, B. H.; Stevenson, J. M.; VandenHeuvel, W. J. A. Fate of avermectin B_{1a} in soil and plants. *J. Agric. Food Chem.* **1984**, *32*, 94–102.

Chiu, S-H. L.; Taub, R.; Sestokas, E.; Lu, A. Y. H.; Jacob, T. A. Comparative in vivo and in vitro metabolism of ivermectin in steers, sheep, swine, and rat. *Drug Metab. Rev.* **1987**, *18*, 289–302.

Chiu, S-H. L.; Carlin, J. R.; Taub, R.; Sestokas, E.; Zweig, J.; VandenHeuvel, W.J. A.; Jacob, T. A. Comparative metabolic disposition of ivermectin in fat tissues of cattle, sheep, and rats. *Drug Metab. Dispos.* **1988**, *16*, 728–736.

Crouch, L. S.; Feely, W. F.; Arison, B. H.; VandenHeuvel, W. J. A.; Colwell, L. F.; Stearns, R. A.; Kline, W. F.; Wislocki, P. G. Photodegradation of avermectin B_{1a} thin films on glass. *J. Agric. Food Chem.* **1991**, *39*, 1310–1319.

Crouch L. S.; Gordon, L. R.; Feely, W. F.; Maynard, M. S.; Wise, L. D.; Wislocki, P. G. Nontoxicity of polar abamectin degradates from citrus fruit and thin film photolysis. *J. Agric. Food Chem.* **1992**, *40*, 88–92.

Feely, W. F.; Wislocki, P. G. Avermectin B_{1a} in celery: acetone-unextractable residues. *J. Agric. Food Chem.* **1991**, *39*, 963–967.

Feely, W. F.; Crouch, L. S.; Arison, B. H.; VandenHeuvel, W. J. A.; Colwell, L. F.; Wislocki, P. G. Photodegradation of 4″-(Epimethylamino)-4″-deoxyavermectin B_{1a} thin films on glass. *J. Agric. Food Chem.* **1992**, *40*, 691–696.

Haque, A.; Weisgerber, I.; Klein, W. Butron-^{14}C bound residue complex in wheat plants. *Chemosphere* **1976**, *3*, 167–172.

Hendry, G. Why do plants have cytochrome P-450? Detoxification versus defence. *New Phytol.* **1986**, *102*, 239–247.

Honeycutt, R. C.; Adler, I. L. Characterization of bound residues of nitrofen in rice and wheat straw. *J. Agric. Food Chem.* **1975**, *23*, 1097–1101.

Maynard, M. S.; Iwata, Y.; Wislocki, P. G.; Ku, C. K.; Jacob, T. A. Fate of avermectin B_{1a} on citrus fruits: 1. Distribution and magnitude of the avermectin B_{1a} and ^{14}C residue on citrus fruits from a field study. *J. Agric. Food Chem.* **1989a**, *37*, 178–183.

Maynard, M. S.; Gruber, V. G.; Feely, W. F.; Alvaro, R.; Wislocki, P. G. Fate of the 8,9-*Z* isomer of avermectin B_{1a} in rats. *J. Agric. Food Chem.* **1989b**, *37*, 1487–1491.

Maynard, M. S.; Wislocki, P. G.; Ku, C. K. Fate of avermectin B_{1a} in lactating goats. *J. Agric. Food Chem.* **1989c**, *37*, 1491–1497.

Maynard, M. S.; Halley, B. H.; Green-Erwin, M.; Alvaro, R.; Gruber, V.; Hwang, S-C.; Bennett, B.; Wislocki, P. G. Fate of avermectin B_{1a} in rats. *J. Agric. Food Chem.* **1990**, *38*, 864–870.

MK244 Technical Data Sheet, Merck Sharp & Dohme Research Laboratories, Three Bridges, NJ.

Moye, H. A.; Malagodi, M. H.; Yoh, J.; Deyrup, C. L.; Chang, S. M.; Leibee, G. L.; Ku, C. K.; Wislocki, P. G. Avermectin B_{1a} metabolism in celery: a residue study. *J. Agric. Food Chem.* **1990**, *38*, 290–297.

Quistad, G. B.; Menn, J. The disposition of pesticides in higher plants. In *Residue Reviews*; Gunther, F. A., Gunther, J. D., Eds.; Springer-Verlag: Berlin, 1983; Vol. 85, pp 173–197.

Shimabukuro, R. H.; Lamourex, G. L.; Frear, D. S. Pesticide metabolism in plants. Reactions and mechanisms. In *Biodegradation of Pesticides*; Matsumura, Murti, Eds.; Plenum Press: New York, 1982; Chapter 2.

Trumble, J. T.; Moar, W. J.; Babu, J. V.; Dybas, R. Laboratory bioassays of the acute and antifeedant effects of avermectin B1 and a related analogue on *Spodoptera exigua* (Hubner). *J. Agric. Entomol.* **1987**, *4*, 21–28.

Received for review April 28, 1995. Accepted August 28, 1995.[⊗]

JF950255+

[⊗] Abstract published in *Advance ACS Abstracts,* October 15, 1995.